



A THERMAL CONDUCTIVITY MODEL FOR RUBBERISED MORTAR

S. Yang (1), N. Ukrainczyk (1) and E. A. B. Koenders (1)

(1) Institute of Construction and Building Materials, Technische Universität Darmstadt,
Franziska-Braun-Straße 3, 64287 Darmstadt, Germany

<https://doi.org/10.21452/bccm4.2018.02.02>

Abstract

The study reported in this paper was done with the aim to investigate the effective thermal conductivity of crumb-rubber-modified mortar through a numerical way. Crumb rubber with the particle size (1-2 mm) was used to replace 5%, 7.5%, 10%, 12.5%, and 15% of the volume of quartz sand with the same size. A numerical simulation method for heat transfer at the meso-scale level of this composite material was applied to model the meso-structure of this composite material, with emphasis on the random packing of spherical particles, volume fractions, and particle size distributions (PSDs), for each component, i.e. rubber, quartz sand and air. A representative volume element (RVE model) was generated using an implicit finite difference method to solve the three-dimensional heat transport equation. In fact, the effective thermal conductivity was strongly depending on the thermal conductivities of all individual solid components. From this, a parameter estimation method was applied whereby the Levenberg-Marquardt algorithm was implemented in MatLab. Simulation results were validated by comparison with literature data. Using the estimated parameters, the effective thermal conductivity of mortar, including the effect of crumb rubber replacement, was presented. Comparison indicated that good agreement existed between the present simulations and the experimental results.

1. INTRODUCTION

In order to effectively reduce the environmental impact caused by the rapid increase of waste rubber tires, mixing its crumb rubber flacks into cementitious materials will immobilize these environmental pollutants and turning it into a green resource in a practical and sustainable way. Several previous studies proved that the addition of rubber particles may significantly reduce the effective thermal conductivity (ETC) of these cement-based composites [1][2][3][4][5]. However, numerical modelling results of this material are yet very scarce in the literature. Nevertheless, some numerical simulations in terms of heat transfer in composite and porous materials may serve as valuable reference for this study.

Coquard and Baillis [6] investigated the conductive heat transfer through heterogeneous cellular materials using a numerically finite volume method based on a meso-structure, which was obtained through X-ray tomography. Wang and Pan [7] solved a thermal energy transport equation for an open-cell foam structure by using a highly-efficiency lattice Boltzmann

method. She et al. [8] presented a random generation method to generate microstructures of foamed concretes, and used a finite volume method to simulate the heat transfer through porous structures. Hui et al. [9] determined ETCs of graded composites by means of a finite element method approach. Based on previous work, in this study a numerical model for determination of ETC of rubberised mortar was developed. Moreover, an inverse identification method for parameters estimation was proposed as well.

2. NUMERICAL APPROACH FOR DETERMINATION OF ETC

The starting point for the modelling is that spherical particles are randomly positioned inside a predefined volume representing an initial cement paste matrix, while following particles size distribution (PSD) for each component: rubber, quartz sand and air. The process began with stacking the larger particles, subsequently followed by smaller ones. Particle size distributions of crumb rubber and quartz sand are measured through Horiba LA-950 Laser Diffraction Particle Size Analyser, which is approximated by the following Rosin-Rammler function

$$G(x) = 1 - \exp(-b * x^n), \quad (1)$$

where $G(x)$ is the particle cumulative weight (g) with diameter x (mm), and with b and n being constants representing the shape of the grading curve.

The basic principle of the developed conductivity model is Fourier's first law of heat conductivity, which can be expressed as:

$$Q_x = -\lambda A \frac{\partial T}{\partial x}, \quad (2)$$

where, Q_x (W) is the heat flow rate by a conductivity λ (W/mK), which is the thermal conductivity of a material, A (m²) is the cross-sectional area normal to the gradient $\partial T/\partial x$ (K/m), which is the derivative of temperature with respect to the x -direction. The negative sign in Fourier's equation indicates that the heat flows in the direction of a decreasing temperature. When Fourier's law is combined with the law of thermal energy conservation, a one dimensional heat conduction equation can be expressed as:

$$\frac{\partial^2 T}{\partial x^2} + \frac{E_b}{\alpha} = \frac{1}{\alpha} \frac{\partial T}{\partial t}, \quad (3)$$

where, $\alpha = \lambda / (\rho * C_p)$ (m²/s).

In case of a steady state heat conductivity problem, when the heat flow takes place in three dimensions, and there is no internal heat generation, equation (3) expands to the Laplace's equation:

$$\lambda_x \frac{\partial^2 T}{\partial x^2} + \lambda_y \frac{\partial^2 T}{\partial y^2} + \lambda_z \frac{\partial^2 T}{\partial z^2} = 0. \quad (4)$$

When considering heat transfer through a porous medium (in z -direction), this is only possible when the heat gradient goes from the warm surface to the colder surface, which also holds for a regular cement paste. When the other four sides of the representative volume are isolated (see Figure 1), a true one dimensional heat flow will occur in the sample. According to this, the boundary conditions are given as follows:

$$\left. \frac{\partial T}{\partial x} \right|_{x=0} = \left. \frac{\partial T}{\partial x} \right|_{x=L} = 0; \quad \left. \frac{\partial T}{\partial y} \right|_{y=0} = \left. \frac{\partial T}{\partial y} \right|_{y=L} = 0, \quad (5)$$

$$T|_{z=0} = T_{\text{hot}}, T|_{z=L} = T_{\text{cold}}. \quad (6)$$

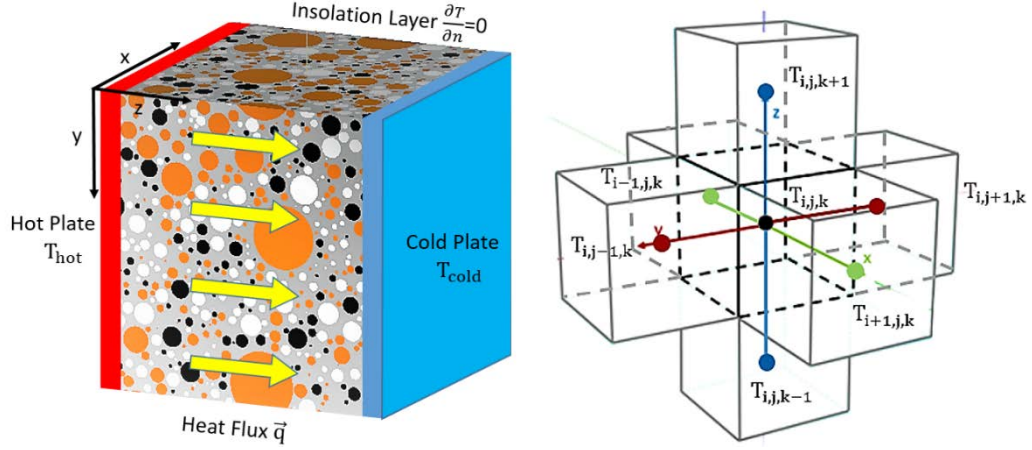


Figure 1: Illustration of the principle of the ETC modelling

The lattice points represent the each component with a different thermal conductivity. In order to establish the connection between two adjacent points, the thermal conductivity in the middle of two points can be expressed as:

$$\lambda_m = 2 / \left(\frac{1}{\lambda_i} + \frac{1}{\lambda_{i+k}} \right), \quad (7)$$

where $k=1$ (in x -direction), L (in y -direction) or L^2 (in z -direction). L represents the number of voxels in a row.

Each lattice point exchanges heat with six neighbouring lattices points (see Figure 1, right). According to the energy balance principle, the sum of the heat that flows into the lattice should be equal to the heat that flows out of the lattice. The equation with all lattice points can be represented in a matrix form as follows:

$$A\mu = b, \quad (8)$$

where the matrix μ is a space-matrix vector and A is a sparse symmetrical matrix, which corresponds to the temperatures of all unknown lattice points, b is a vector, which represents the boundary conditions of the system.

The heat flow through each point along the z -axis can be calculated as:

$$q_{i,z} = \frac{1}{2} [(\mu_{i-L} - \mu_i)\lambda_{z,i-L} + (\mu_i - \mu_{i+L})\lambda_{z,i}]. \quad (9)$$

Owing to the microstructure of rubberised cement-based composite regarded as an equivalent continuous medium, the effective thermal conductivity λ_i of the composite is equal to the effective thermal conductivity $\lambda_{i,z}$ calculated in z -direction.

$$\lambda_i = \lambda_{i,z} = -\frac{Q_z}{L^3} * \left(\frac{L+1}{T_{\text{hot}} - T_{\text{cold}}} \right). \quad (10)$$

3. MATERIALS AND EXPERIMENTAL TESTING

Materials used in this study consist of the Portland cement CEM I 42.5R (HeidelbergCement company), crumb rubber (Genan A/S company), quartz sand (Euroquartz company), water and superplasticiser (Sika® ViscoCrete). Three particle sizes of sand were used: 0.1-0.5 mm, 0.5-1.0 mm and 1.0-2.0 mm. The crumb rubber with particles size of 0.8-2.0 mm was obtained through the ambient grinding process. Crumb rubber replacement levels were set to 5%, 7.5%, 10%, 12.5% and 15% by volume of quartz sand, respectively. As for the mix proportion, the water-cement ratio was set to 0.45. The detailed mix design of rubberized mortar and reference mortar are presented in Table 1.

Table 1: Mix design

No.	crumb rubber (vol.-%)	w/c	cement (kg/m ³)	water (kg/m ³)	crumb rubber (kg/m ³)	quartz sand (kg/m ³)			superplasticiser (kg/m ³)
						0.1-0.5	0.5-1.0	1.0-2.0	
REF	0	0.45	550	245.7	0	563.52	290.62	440.49	1.93
CR_2.0a	5	0.45	550	245.7	59	563.52	290.62	309.74	1.93
	7.5				88.5			244.37	
	10				118			178.99	
	12.5				147.5			113.62	
	15				177			48.24	

For each mixture, three samples of 40x40x160 mm³ prisms were prepared and cured in water at 20±1 °C. The specimens were dried at the age of 28 days in an oven at 45 °C and weighed at 24 h intervals until the loss in weight did not exceed 0.2% in 24 hours. The TPS instrument (manufactured by Hot Disk AB) was used to measure the effective thermal conductivity of mortar specimens at 20 °C. For each specimen, three measurements were performed.

4. STATISTICAL EVALUATION OF REPRESENTATIVE ELEMENT VOLUME

4.1 Concept of REV

A cement-based material is a heterogeneous system, which consists of a solid matrix and a complex pore system. To describe a heterogeneous system, as suggested by Bear [10], this can be done by introducing the concept of representative elementary volume (REV). In this study, a REV was determined through a statistical analysis of simulations [11]. Several experiments of increasing sizes of the microstructure were conducted, and for each microstructure different particles' position and voxel resolution were considered. Then the chi-square statistic was applied for determining the size of the REV.

$$\chi^2 = \frac{\sum_{i=1}^m (\lambda_i - \lambda_a)^2}{\lambda_a} \quad (11)$$

in this, λ_i is the investigated thermal conductivity of current microstructure, which is calculated from Equation (10). λ_a is the average of all λ_i and m is the number of realisations for the current rib size. This procedure demonstrates that the smaller the value of χ^2 is, the closer is the volume of the respective sample to the expected REV. In spite of this, a sample with a smaller volume can be generally used when the value of χ^2 is acceptably low. In this study, 0.1 is used as an acceptable value, and the degree of freedom is 1 which is the random distribution of particles. This means that if χ^2 is lower than 0.1, there is at least a 95% chance probability confidence that the visual particle structure can be regard as REV.

4.2 Determination of REV and results analysis

The tests were conducted with several rib sizes from 30 mm to 200 mm. For each rib size, three voxel resolutions were analysed: 1 pixels/mm, 2 pixels/mm and 4 pixels/mm. For each rib size and each voxel resolution, five visual microstructures were generated. A total of 105

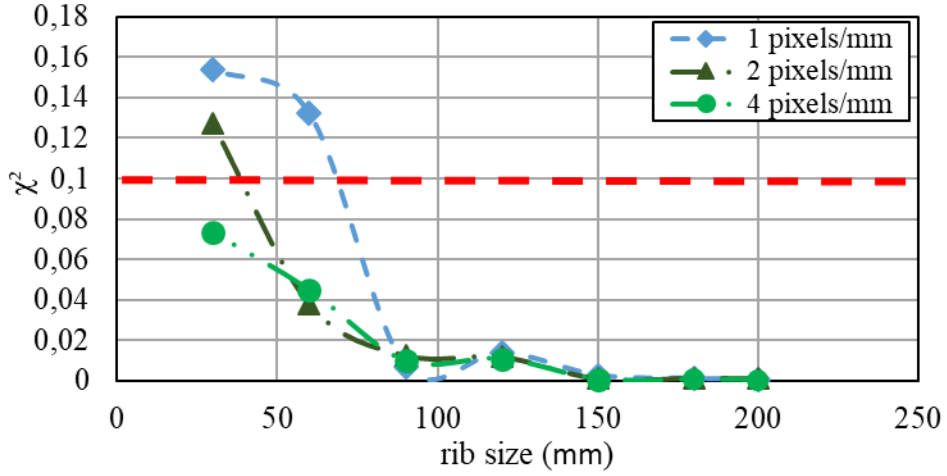


Figure 2: statistical analysis of REV

numerical tests were performed. The determination procedure was carried out with C++ language using GNU Compiler Collection (GCC 6.3.0) on a high-performance computer at TU-Darmstadt Lichtenberg (12 cores, 5900 TFlops/s, Intel Xeon E5-2670 Sandy Bridge). In order to improve the efficiency of used of computer memory and speed up the implementation of the procedure, a parallel computing scheme was achieved through Open Multi-Processing (OpenMP 2.0.1). The results of the REV size determination are presented in Figure 2. When a chi-squared value of 0.1 is acceptable with a probability of at least 95%, then the rib size of the microstructure of the mortar to establish the REV should be larger than 90 mm (1 pixels/mm), 60 mm (2 pixels/mm) and 30 mm (4 pixels/mm). The results of this analysis were applied for predicting the effective thermal conductivity and parameter estimation in the following sections.

5. INVERSE APPROACH FOR PARAMETER ESTIMATION

Based on an actual experimental investigation on a composite, the thermal conductivities of its components can be estimated by minimising the deviation between simulated and experimental data. The objective function is expressed as follows:

$$\min F(\lambda_i) = [\lambda_{\text{sim}}(\lambda_i) - \lambda_{\text{exp}}]^T [\lambda_{\text{sim}}(\lambda_i) - \lambda_{\text{exp}}], \quad (12)$$

where $F(\lambda_i)$ represents a non-linear function of the parameters, $\lambda_{\text{sim}}(\lambda_i)$ is the effective thermal conductivity of a composite, which is calculated based on the thermal conductivities of components and their spatial distributions. λ_{exp} is the experimental value. The unknown parameter λ_i is obtained and can minimise the objective function. A Levenberg-Marquardt algorithm [12][13] of the MatLab Optimisation Toolbox was used to estimate the thermal conductivity of quartz sand and rubber. The step tolerance (TolX) and the function tolerance (TolFun) were set to the same value 1e-3. However, this method cannot guarantee to find the global minimum. Therefore, different initial points were test in order to achieve good coverage on optimal solutions. A cube with the side length of 90 mm and with the voxel resolution of 1 pixels/mm was chosen as the representative elementary volume (REV) of an agar- quartz sand/rubber structure (see Figure 3). In order to determine the air void content, a

compress equalisation method was adopted, by which a TESTING air entrainment meter was used. During the measurement, agar was in liquid state.

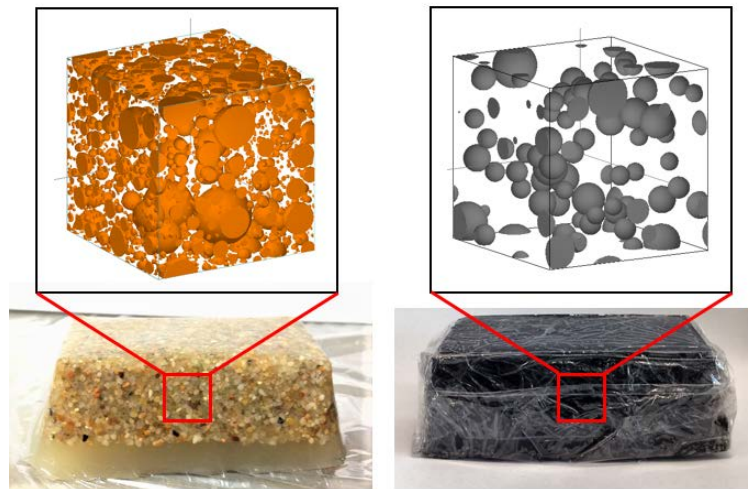


Figure 3: View of ETC of agar- quartz sand/rubber samples and numerical meso-structures.

6. SIMULATION RESULTS AND ANALYSIS

The results show that the effective thermal conductivity of agar- quartz sand and agar-rubber sample is 2.563 (W/mK) and 0.485 (W/mK) with the corresponding air void content 0.21 vol.-% and 3.0 vol.-%, respectively. The estimated thermal conductivity of quartz sand and rubber particle is 4.420 (W/mK) and 0.214 (W/mK), respectively.

Due to different chemical compositions, the estimated thermal conductivity of rubber is slightly higher than the value in literature (from 0.13 to 0.19 W/mK [2][22][23][24][25]). Furthermore, since the thermal conductivity of quartz sand is strongly depending on the quartz content and moisture content [14][15][16][21], and measurement approaches are various, the literature shows a wide range of variation. In the study of Côté & Konrad [16], the result was summarised from nearly 1000 test results in the literature. Kersten [15] performed an extensive series of tests on different types of quartz sand. The comparison of the parameter estimation results and the values from published literature is shown in Figure 4.

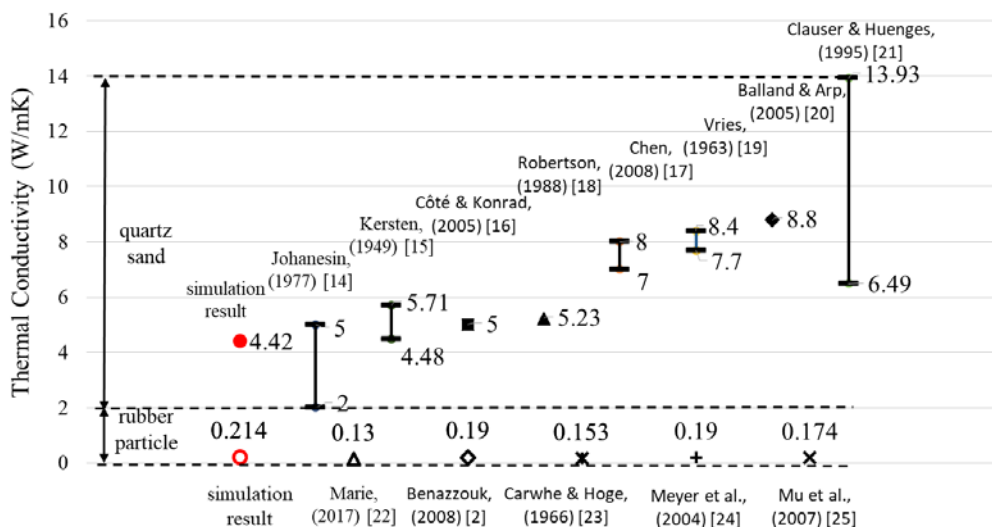


Figure 4: Parameter estimation results and literature survey of thermal conductivity of quartz sand and rubber

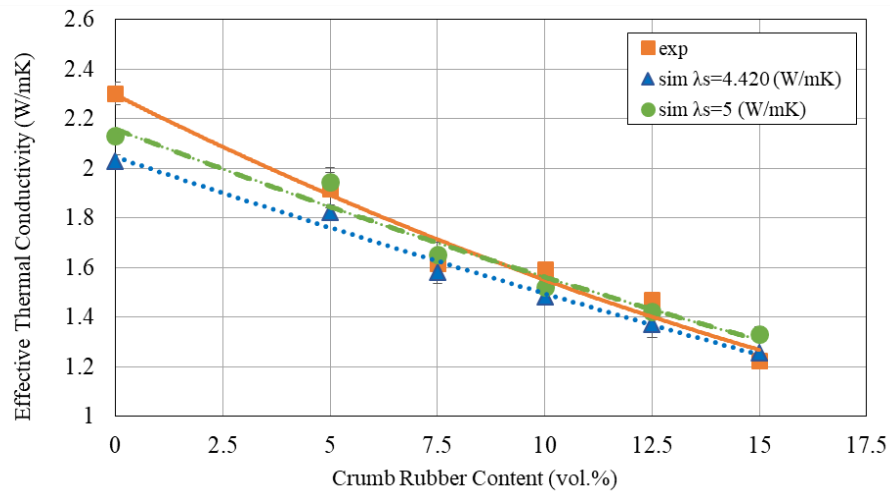


Figure 5: Effect of crumb rubber content on thermal conductivity of mortar

Notably, the thermal conductivity of quartz sand is much higher than that of rubber. Only a minor deviation of thermal conductivity of quartz sand can lead to a significant change of the ETC of mortar. Thus, it is very crucial to ensure a suitable accuracy of simulation results. In the following numerical experiment, two values of quartz sand (4.420 W/mK and 5 W/mK from the literature) were tested. The thermal conductivity of cement paste with a 0.45 w/c ratio at 28-days was measured through the hot disk method, its value is 0.685 (W/mK). The thermal conductivity of air 0.026 (W/mK) is taken from the literature [26][27]. For each sample, 6 simulation estimations were performed. The predicted parameter was produced by the average of all results. The comparisons of the simulation results with the experimental data in terms of the impact of crumb rubber content on the ETC of mortar are illustrated in Figure 5.

A decreasing tendency of the effective thermal conductivity of mortar with the increase in crumb rubber content and air void content was described using a second order polynomial, respectively. The experimental results show that by replacing quartz sand with crumb rubber at 5% to 15%, the effective thermal conductivity of mortar was reduced from 17% up to 47%. This is not only due to increased air void content from 5% to 12%, but also because the thermal conductivity of crumb rubber is much lower than that of quartz sand. Moreover, it can be deduced from Figure 5 that when a tipping point of crumb rubber content is reached, the ETC of mortar will not decrease anymore. It is mainly because of a reduction in the workability with increasing crumb rubber content. Since the air bubbles are formed in the cement paste, a reduction of the workability of mortar makes it hard to entrain air in the cement past.

By using the estimated thermal conductivity of quartz sand (4.420 W/mK), the results are slightly lower than the experimental results. When the thermal conductivity of sand is increased to 5 (W/mK) and the other parameters stay constant, the results get much closer to the experimental results. The average differences of two ETC simulation results are 5.88% and 4.12 %, respectively.

The error originates mainly from the air void content of the agar- quartz sand sample in the liquid state measured through a compress equalisation method. This method is based on Boyle's law 0, which states that the volume occupied by a given mass of gas is proportional to the applied pressure. If the sample is entrained with a large amount of small air bubbles, they will not register a change in pressure. Therefore, the air void content of agar- quartz sand sample determined through this method is less than the actual value, which leads to the predicted thermal conductivity of quartz sand to be smaller than the values in the literature,

lowering the simulated ETC of mortar. This trend is considerably more pronounced when the mortar contains more quartz sand, like the reference mortar. Therefore, a more accurate approach is required.

7. CONCLUSION

A meso-scale numerically modelling is developed for predicting the effective thermal conductivity of rubberised mortar. The effective thermal conductivity of heterogeneous material is described via the concept of representative volume elements. When a chi-squared value of 0.1 is regarded as an acceptable value, the REV should be larger than 90 μm (1 pixels/ μm), 60 μm (2 pixels/ μm) or 30 μm (4 pixels/ μm).

A Levenberg-Marquardt algorithm was used to estimate the thermal conductivity of quartz sand and rubber particle based on measurement results of agar- quartz sand/rubber sample. The estimation results are within the range of values from the literature. Moreover, the simulated ETCs of rubberised mortars are in good agreement with the experimental results. When the thermal conductivity of quartz sand 5 (W/mK) instead of 4.420 (W/mK) was adopted, which proved a better approximation of experimental results.

ACKNOWLEDGEMENTS

The authors would like to thank the contributors of laboratory of the institute of Construction and Building Materials of the TU Darmstadt.

REFERENCES

- [1] Herrero, S., et al., 'Influence of proportion and particle size gradation of rubber from end-of-life tires on mechanical, thermal and acoustic properties of plaster-rubber mortars', *Materials & Design*. **47** (2013) 633–642.
- [2] Benazzouk, A., et al., 'Thermal conductivity of cement composites containing rubber waste particles', *Construction and Building Materials*. **22** (4) (2008) 573–579.
- [3] Sukontasukkul, P., 'Use of rubber to improve thermal and sound properties of pre-cast concrete panel', *Construction and Building Materials*. **23** (2) (2009) 1084–1092.
- [4] Najim, K. B. and Hall, M. R., 'Workability and mechanical properties of crumb-rubber concrete', *Construction Materials*. **166** (1) (2013) 7–17.
- [5] Marie, I., 'Thermal conductivity of hybrid recycled aggregate – Rubberized concrete', *Construction and Building Materials*. **133** (2017) 516–524.
- [6] Coquard, R. and Baillis, D., 'Numerical investigation of conductive heat transfer in high porosity foams', *Acta Materialia*. **57** (18) (2009) 5466–5479.
- [7] Wang, M. and Pan, N., 'Modeling and prediction of the effective thermal conductivity of random open-cell porous foams', *Int. Journal of Heat and Mass Transfer*. **51** (5-6) (2008) 1325–1331.
- [8] She, W., et al., 'Three-dimensional numerical modeling and simulation of the thermal properties of foamed concrete', *Construction and Building Materials*. **50** (2014) 421–431.
- [9] Hui, P.M., Zhang, X., Markworth, A.J. et al., 'Thermal conductivity of graded composites: Numerical simulations and an effective medium approximation', *Journal of Materials Science*. **34** (1999) 5497-5503.
- [10] Bear, J., 'Dynamics of Fluids in Porous Media', New York, Dover Publ. (1972).
- [11] Gitman, M. B. and Askes, H., 'Quantification of stochastically stable representative volumes for random heterogeneous materials', *Archive of Applied Mechanics*. **75** (2006) 79–92.
- [12] Moré, J. J., 'The Levenberg-Marquardt Algorithm: Implementation and Theory', Numerical Analysis, ed. G. A. Watson, Lecture Notes in Mathematics 630, Springer Verlag. (1977) 105–116.

- [13] Henri, P. G., 'The Levenberg-Marquardt method for nonlinear least squares curve-fitting problems', North Carolina, USA. (2013).
- [14] Johannesin, O., 'Thermal conductivity of soils', Ph. D. thesis, Trondheim, Norway. (1977).
- [15] Kersten, M., S., 'Thermal properties of soils', Ph. D. thesis, University of Minnesota Engineering Experiment Station Bulletin. **28** (1949).
- [16] Côté, J. and Konrad, J. M., 'A generalized thermal conductivity model for soils and construction materials', *Canadian Geotechnical Journal*. **42** (2) (2005) 443-458.
- [17] Chen, S. X., 'Thermal conductivity of sands', *Heat Mass Transfer*. **44** (10) (2008) 1241–1246.
- [18] Robertson, E., C., 'Thermal properties of rocks', *United States Department of the Interior Geological Survey*. (1988) 88–441.
- [19] Vries, D. A. de, 'Thermal properties of soils', *Physics of Plant Environment*. (1963) 210–235.
- [20] Balland, V. and Arp, P. A., 'Modeling soil thermal conductivities over a wide range of conditions', *Environmental Engineering & Science*. **4** (6) (2005). 549–558.
- [21] Clauser, C. and Huenges, E., 'Thermal conductivity of rocks and minerals', *Rock Physics and Phase Relations*. (1995) 105–126.
- [22] Marie, I., 'Thermal conductivity of hybrid recycled aggregate – Rubberized concrete', *Construction and Building Materials*. **133** (2017) 516–524.
- [23] CarwHe, L. C. K. and Hoge, H. J., 'Thermal conductivity of soft vulcanized natural rubber: selected values'. (1966).
- [24] Meyer, L., et al., 'Thermal conductivity of filled silicone rubber and its relationship to erosion resistance in the inclined plane test', *IEEE Transactions on Dielectrics and Electrical Insulation*. **11** (4) (2004) 620–630.
- [25] Mu, Q. H., et al., 'Thermal conductivity of silicone rubber filled with ZnO', *Polymer Composites*. **28** (2) (2007) 125–130.
- [26] Kadoya, K., Matsunaga, N., Nagashima, A., 'Viscosity and thermal-conductivity of dry air in the gaseous-phase', *J. Phys. Chem. Ref. Data*. **14** (4) (1985) 947-970.
- [27] Montgomery, R. B., 'Viscosity and thermal conductivity of air and diffusivity of water vapour in air'. *J. Meteor*. **4** (1948) 193-196.
- [28] Bonnor, W. B., 'Boyle's law and gravitational instability', *MNRAS*. **116** (351) (1956) 351-359.